

# Vibration isolation system using spring actuator with iron particle layers stacked with permanent magnet and electromagnet under disturbance cancellation control

K. NAGAYA\*, H. HATA, N. SAKAMOTO, A. NOJIRI, I. MURAKAMI

*Department of Mechanical Engineering, Gunma University, Kiryu, Gunma 376-8515, Japan*

---

A new spring type actuator is presented in which controls are possible by using usual control methods such as PID control. The actuator consists of a normal helical coil spring and a number of iron (ferrite) particles layers inside. The iron particles layers are made of silicon based adhesive material involving iron particles. The layers are pasted to the coil spring with a certain air gap between each layer. To achieve both extensive and compressive motions, a permanent magnet is attached to the top of the spring and electromagnet to the base, and the motion of the top of the actuator is controlled by electric currents in the coil of the electromagnet. A method of vibration isolation control is presented using the actuator. In the control, only the disturbance of base is detected, and the disturbance cancellation control is performed. Especially, the system requires no state variables of the vibrating body, and the transmissibility is almost zero in wide frequency ranges.

(Received March 13, 2008; accepted May 5, 2008)

*Keywords:* Spring, Actuator, Electromagnet, Iron particles layer, Vibration Isolation, Control

---

## 1. Introduction

Recently, high-speed linear actuators have been developed, and applied to position and vibration control problems. As for high-speed actuators, piezoelectric and magneto-strict actuators are now in practical use, but their displacements are significantly small, and so their applications are limited in some special devices. Although large displacements are possible in using shape memory alloy actuators, the response speed of the actuators is slow, and a cooling mechanism is required to have rapid response [1]-[3]. A moving coil actuator has been used for having large displacements and rapid response [4], but it requires a magnet, magnetic circuit, moving coil, coil bobbin and spring, and so its size is large in general. An electromagnet will be able to generate a large force under electric currents because of using magnetic moments of iron. Since its force is in proportion to an inverse of square of air gap, the size is also big, because it requires a strong magnet with electric circuits and spring for having large displacement operation. Moreover, it cannot control both positive and negative displacements because of its force being only in one direction (an attractive force).

The object of the present paper is to develop a compact actuator under electromagnetic control, which has no disadvantages mentioned above. In order to delete disadvantages of the electro magnet, the present actuator consists of a number of iron particles layers, which are pasted along a spring coil.

The air gaps between iron layers are small, and so large electromagnetic forces act on the layers, but the total displacement becomes large because the displacement is given by the superposition of small displacements of iron layers. The size of the actuator is compact in comparison

with other actuators in which a large displacement is required. Although the compressive displacement is possible in the actuator, the extension displacement cannot be obtained. To have both operations of compression and extension, a permanent magnet is attached at the top of the spring. The spring is compressed by the permanent magnet, and a further compression is given by the electromagnet with currents, which increases the magnetic flux density. In the actuator, the magnetic flux can be decreased by the opposite direction current in the electromagnet, and the extension operation is obtained by the restoring force of the spring and the repulsive magnetic forces. Therefore, both operations of compression and extension are possible in this actuator. Since the mass of the actuator will be small in comparison with moving coil actuators, and electromagnetic actuators, the response speed will be rapid, and operation displacements are larger than the high speed actuators such as magneto-strict- and piezoelectric-actuators.

The actuator developed in this article is applied to a vibration isolation device, in which disturbances of the base is only detected, and the disturbance forces are canceled by using the actuator. In usual vibration isolation control, displacement and velocity of the vibrating body were detected, and vibrations were controlled to be minimum by using a certain control method, but in which the maximum transmissibility is greater than one in the frequency response. The technique used in this article is based on our previous work [5], but the method is different from them. Although our previous method is straightforward and the control device is compact, it requires the velocity of vibrating body to suppress resonance peaks, and so the control device is still complex. In the present article, the control system is compact in

comparison with our previous system, because the displacement of the base is only required. Therefore, both mechanism and control system are compact; in addition the transmissibility is almost zero (the maximum transmissibility is less than one) in the frequency response when the present system is used.

**2. Development of spring actuator**

Fig. 1 shows the geometry of the spring actuator presented in this article. It consists of coil spring B made of non-magnetic material such as stainless steel in which a number of iron particles layers F are stacked, electromagnet C, and permanent magnet A. To make iron particles layers, ferrite particles with 20 through 50 μm in diameter and silicon based paste are mixed together. The mixed particles and styrene foam are sandwiched by turns inside the coil spring, and heated at 160 °C in a furnace. In the operation, the styrene vanishes during the heating and air gap E is created, and the coil spring having iron particles layers is formed, because the silicon, which becomes silicon rubber during the heating, is pasted along the coil spring. In order to have compression and extension displacements, a permanent magnet lies at the top, and an electromagnet at the base of the spring.

Table 1. Dimensions of the coil for the electromagnet.

|                            |      |      |
|----------------------------|------|------|
| Inner diameter of the coil | [mm] | 56   |
| Height of the coil         | [mm] | 20   |
| Wire diameter              | [mm] | 0.75 |
| Outer diameter of the coil | [mm] | 91   |
| Number of turns            |      | 559  |
| Electrical resistance      | [Ω]  | 5    |
| Diameter of center hole    | [mm] | 15   |

The coil spring has a helical shape and perpendicular forces to the axis of spring act, so that a slider made of stainless steel in slider hole D is attached in a center of the spring. When electric currents act on the coil of the electromagnet, the magnetic flux density varies, and magnetic forces act among the iron particles layers, which moves the spring in an axial direction.

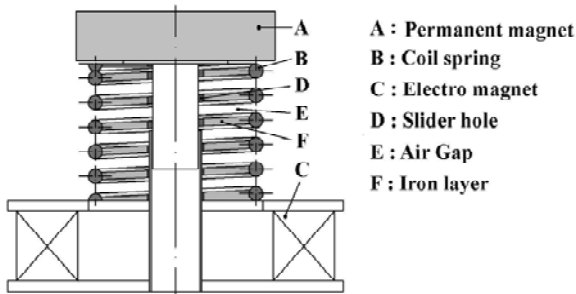


Fig. 1. Geometry of the spring actuator.

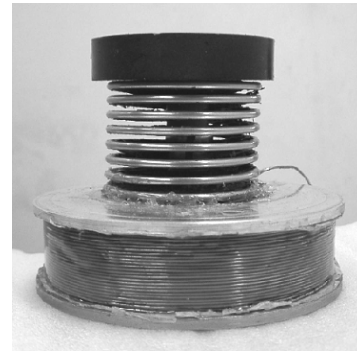


Fig. 2. Photo of spring actuator made in this study.

Table 2. Dimensions of the spring.

|                                 |                      |        |
|---------------------------------|----------------------|--------|
| Outer diameter of spring        | [mm]                 | 48     |
| Wire diameter                   | [mm]                 | 2.4    |
| Length of the spring            | [mm]                 | 39     |
| Number of the effective turns   |                      | 7      |
| Material                        |                      | SUS304 |
| Mass of spring with iron layers | [g]                  | 42     |
| Shear modulus of coil spring    | [N/mm <sup>2</sup> ] | 68,500 |
| Mass of PM with slider          | [g]                  | 150    |

Table 1 depicts the dimensions of the electromagnet and Table 2 the dimensions of the spring made in this study. When electric currents act on the magnet, only attractive forces act in the axial direction, and the spring is compressed. Therefore, it is difficult to have extension displacement. In addition, the frequency of the actuator is twice of the input current frequency under a sinusoidal excitation. This means that a usual control such as PID control cannot be utilized in the actuator. To have both displacements of extension and compression, a permanent magnet lies on the top of the spring. In the system, when the current makes the magnetic flux density created by the permanent magnet increase, the spring moves in the direction of compression, and when the current makes the flux density decrease, the spring is extended due to the restoring force of the spring and repulsive magnetic forces, in which the current frequency is corresponding to the actuator frequency. This means that the present actuator is controlled by usual PID control method. Fig. 2 shows the photograph of the actuator made in the present study.

**3. Application of the actuator to vibration isolation control**

**3.1 Characteristics of the actuator**

Consider a vibration isolation system in which vibrating body is supported by the spring actuator as shown in Fig. 3, where  $m_p$  is the mass of vibrating body,

$C_a$  the damping coefficient,  $k$  the spring constant of the actuator,  $m_s$  the mass of the spring actuator involving iron particles layers.

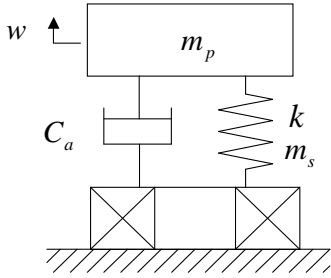


Fig. 3. Vibration isolation system.

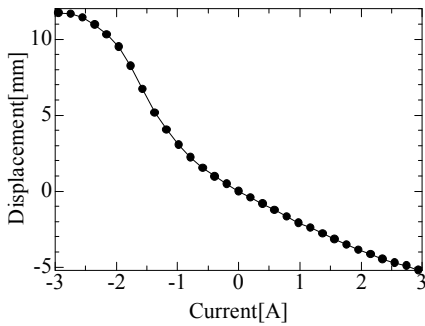


Fig. 4. Displacement versus currents.

The relation between the measured displacements and input currents for the actuator made in this study is shown in Fig. 4. It can be seen that there are large nonlinear characteristics in the figure. However, in the vibration isolation system, amplitudes of base displacements are less than 1 mm, and so we consider the range between  $-1\text{A}$  and  $+1\text{A}$  in the figure. In such a region, a linear approximation is applicable:

$$F(I) = k\varepsilon I \quad (1)$$

where  $F$  is the electromagnetic force acting on the vibrating body,  $\varepsilon$  the constant, and  $I$  the electric current in the electromagnet.

Fig. 5 and 6 show the response of the vibrating body under the sinusoidal excitation of the electromagnetic force of the actuator. Although the displacement in the positive direction (compression) is somewhat greater than that in the negative direction (extension) in low frequency ranges (see Fig. 5), displacements in both positive and negative ranges are almost the same. In addition, the shape of wave is close to that of the harmonic wave. Therefore, vibrations may be controlled by the actuator based on the linear approximation when the amplitudes being less than 1mm.

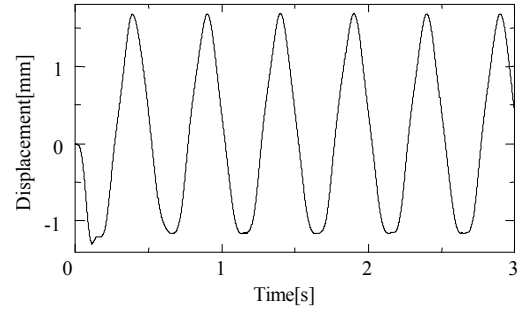


Fig. 5. Time response of the displacement of the vibrating body under sinusoidal excitation  $V=3\sin 4\pi$  [V] in the magnet.

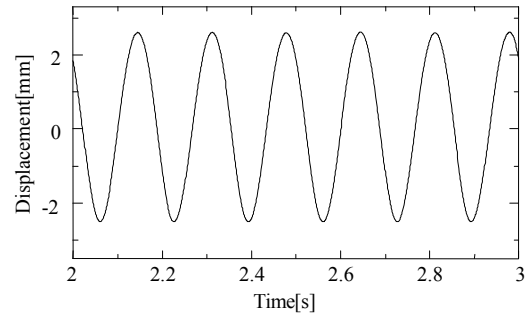


Fig. 6. Time response of the displacement of the vibrating body under sinusoidal excitation  $V=3\sin 12\pi$  [V] in the magnet.

### 3.2 Principle of vibration isolation using the disturbance cancellation

It is difficult to suppress the transmissibility (=amplitude of vibrating body/base amplitude) to be less than one in the low frequency range (less than the first resonance frequency) when a normal feedback control is applied. To suppress the transmissibility to be less than one, we developed the method of disturbance cancellation [5], but in which both the base displacement and the state variables of vibrating body were needed, and the control system was complex because it required the sensors for detecting the displacements or velocity of both the base and vibrating body. In the present article, a new system is developed, which requires a sensor for detecting the base displacement only.

The equation of motion of the system shown in Fig. 3 under the base excitation  $u = u_0 \sin \omega t$  is

$$m_a \frac{d^2 w}{dt^2} + C_a \frac{dw}{dt} + kw = C_a \frac{du}{dt} + ku + F(I) \quad (2)$$

where  $w$  is the displacement of the vibrating body, and  $t$  is the time. When the right term of Eq.(2) is zero, vibration will vanish because of the exciting force being zero. The control force  $F(I)$  in such case is

$$F(I) = -C_a \frac{du}{dt} - ku \quad (3)$$

When the actuator generates the electromagnetic force  $F(I)$  in Eq.(3), the amplitude of vibrating body becomes theoretically zero. In this case, since the force  $F$  has no dependence on the displacement or velocity of the vibrating body, no sensor is required for the vibrating body, but the sensor for detecting the displacement of the base is required.

Since it is difficult to perform the disturbance cancellation control perfectly, a few disturbance cancellation errors remain. Effects of the errors are small in the regions except the resonance, but they induce the resonance at the resonance frequency when the damping is small in the system. The resonance peak will be suppressed by the velocity feedback for the vibrating body, but a velocity sensor is required which makes the system complicated and expensive[5]. The object of this study is to construct a straightforward and compact vibration isolation system, which generates no resonance in spite of using no sensor for the vibrating body.

In the disturbance cancellation, the velocity of the base can be calculated by using the signals of the displacement sensor for the base. Then the control force is created by the feedback control:

$$F(I) = -f_2 \frac{du^*}{dt} - f_1 u^* \quad (4)$$

where  $u^*$  is the displacement signal involving disturbance cancellation errors (measurement errors, parameter errors and control errors), and  $f_1$  and  $f_2$  are the feedback coefficients. Let the disturbance cancellation error of the displacement be  $\Delta u = \eta u$ . The measured displacement  $u^*$  is written by

$$u^* = u - \Delta u = (1 - \eta)u \quad (5)$$

where  $u$  is the real displacement of the base. Substituting Eq.(5) into Eq.(2) yields

$$\frac{d^2 w}{dt^2} + 2\mu \frac{dw}{dt} + p^2 w = 2\mu' \frac{du}{dt} + p^2 \eta u \quad (6)$$

where

$$2\mu = \frac{C_a}{m_a}, \quad p^2 = \frac{k}{m_a}, \quad 2\mu' = \frac{C_a - f_2 + f_2 \eta}{m_a}$$

Solving Eq.(6), we have the transmissibility  $T$ :

$$T = \frac{A}{a} = \frac{\sqrt{\{\eta(1-\Omega^2) + 4\zeta\zeta'\Omega^2\}^2 + \Omega^2\{-2\zeta\eta + 2\zeta'(1-\Omega^2)\}^2}}{(1-\Omega^2)^2 + 4\zeta^2\Omega^2} \quad (7)$$

where  $a$  is the amplitude of the displacement of the base

and  $A$  is the amplitude of the vibrating body, and where

$$\Omega = \frac{\omega}{p}, \quad \zeta = \frac{\mu}{p}, \quad \zeta' = \frac{\mu'}{p}$$

When there is no damping ( $\zeta = 0$ ,  $f_2 = 0$ ), and the disturbance cancellation control is perfect ( $\eta = 0$ ), the transmissibility is zero in Eq.(7), but these values are not zero in practice.

The transmissibility at the resonance ( $\Omega = 1$ ) is

$$T_{\Omega=1} = \left( \frac{A}{a} \right)_{\Omega=1} = \frac{\sqrt{4\zeta'^2 + \eta^2}}{2\zeta} \quad (8)$$

The vibration amplitude  $A$  at the resonance is the following when  $\zeta' = 0$

$$A = \frac{a\eta C_a}{2\sqrt{m_a k}} = const \quad (9)$$

This means that there is no resonance in this condition. Therefore, the feedback coefficients which suppresses the resonance are as follows:

$$f_1 = k, \quad f_2 = \frac{C_a}{1-\eta} \quad (10)$$

Using the feedback coefficients in Eq.(10), the resonance phenomena will vanish.

### 3.3 Experimental results

In the experiment, the system shown in Fig.3 lies on a oscillator table which vibrates in a vertical direction, and the displacement of the table is detected by a laser gap sensor. The signal is input to the digital signal processor (DSP), and the control voltage created in DSP is input to the electromagnet passing through a power amplifier. The displacement of vibrating body is also measured by a laser gap sensor and input to DSP, but its signals are not used in the control. The control voltage  $V_c$  which acts on the coil of the electromagnet is decided by Eq.(4) and (10):

$$V_c = K_1 V_m + K_2 \frac{dV_m}{dt} \quad (11)$$

where

$$K_1 = \frac{R}{\varepsilon K_d K_a}, \quad K_2 = \frac{C_a R}{k \varepsilon K_d K_a (1-\eta)}$$

and where  $R$  is the electric resistance of the electromagnet,  $K_a$  the gain of the power amplifier,  $K_d$  the gain of the laser gap sensor, and  $V_m$  the output voltage of the laser gap sensor ( $V_m = K_d u^*$ ). The coefficients used in the

experiment are as follows:  $R=5.1[\Omega]$ ,  $\varepsilon=1.25 \times 10^{-3}[\text{m/A}]$ ,  $K_d=0.25[\text{V/m}]$ ,  $C_a=1.05[\text{N} \cdot \text{s/m}]$ ,  $k=460[\text{N/m}]$ ,  $\eta=0.236$ , where  $C_a$  is obtained experimentally, and  $\eta$  is obtained by using the displacement of the vibrating body under P-control only ( $f_1=k$ ,  $f_2=0$ ). Using these values, one obtains  $K_1=8.83$  and  $K_2=0.026$ .

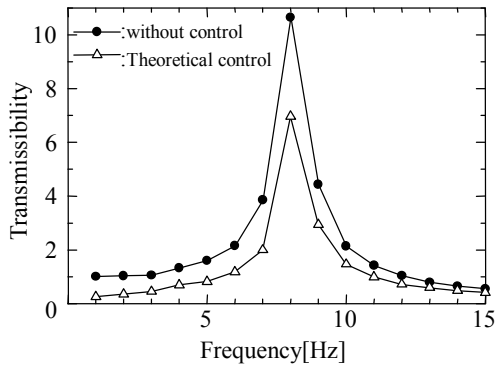


Fig. 7. Comparison between the controlled results with uncontrolled result.

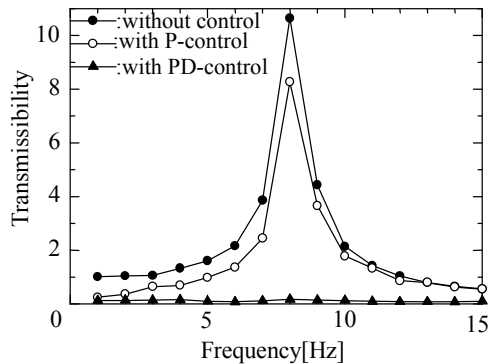


Fig. 8. Comparison between the result under the optimal control and others.

The black circular dots in Fig. 7 and 8 show the transmissibility when the base excitation amplitude  $u$  is 0.43 mm. The transmissibility of the displacement under the theoretical control using the coefficients as just mentioned is shown in Fig. 7 by white triangles. Although the transmissibility under the theoretical control is suppressed in comparison with that of the uncontrolled results, there are still large values in the resonance zone. This will be due to the estimation errors of the system parameters. Therefore, the optimal values were obtained by trial and errors, and the values were found to be  $K_1=8$  and  $K_2=0.18$ . White dots in Fig. 8 depict P-control only using the optimal displacement feedback coefficient  $K_1=8$ , but  $K_2=0$ . The peak value is not suppressed in this case, and so D-control is of importance in this control. Black triangles in Fig.8 show the results under PD optimal

control using  $K_1=8$  and  $K_2=0.18$ . The transmissibility is suppressed remarkably, and resonance phenomena are not observed in this case. Especially the maximum transmissibility is less than one in all frequency ranges, which will be difficult to be achieved in usual PID control.

Figs. 9 and 10 show the time response of the displacement of vibrating body before and after starting the present optimal control. The amplitudes reduce to significantly small values within one second, and the displacement reduction ratios are more than 83%.

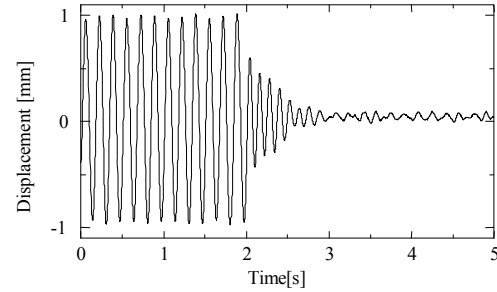


Fig. 9. Response of the vibrating body under the control using optimal feedback coefficients (Exciting frequency = 6Hz).

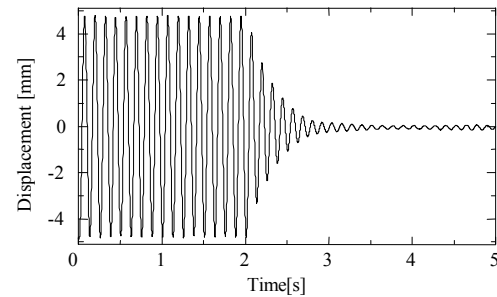


Fig. 10. Response of the vibrating body under the control using optimal feedback coefficients (Exciting frequency = 8Hz).

### 3.4 Method for obtaining the optimal feedback coefficients

As mentioned above, the feedback coefficients will be of importance to suppress vibrations because only the optimal values of the feedback coefficients can control vibrations which are different from those of the usual feedback control. In order to have the optimal values, we consider the following cost function:

$$J = \left( \frac{w(t)_{\max} - w(t)_{\min}}{2} \right) \quad (12)$$

$$J = \left( \frac{w(t)_{\max} - w(t)_{\min}}{2} \right)$$

where  $w(t)_{\max}$  is the maximum displacement and  $w(t)_{\min}$  the minimum displacement of the vibrating body. To have minimum values of the cost function  $J$ , the steepest decent method is applied with respect to the feedback gains  $K_1$

and  $K_2$  as written below:

$$K_{1,i+1} = K_{1,i} - \eta_1 \frac{\partial J}{\partial K_1} \quad (i = 1, 2, 3 \dots) \quad (13a)$$

$$K_{2,i+1} = K_{2,i} - \eta_2 \frac{\partial J}{\partial K_2} \quad (i = 1, 2, 3 \dots) \quad (13b)$$

where  $\eta_1$  and  $\eta_2$  are the coefficients. Repeating the calculation in Eq.(12) to (13) for cycle  $i$ , we have the converged values of  $K_1$  and  $K_2$ . Figs. 11 and 12 show the relations between the coefficients versus the time, and Figure 13 the variation of the control voltage in the electromagnet. The converged values are obtained for about 30 seconds, and obtained values are

$K_1=8.8$  and  $K_2=0.18$

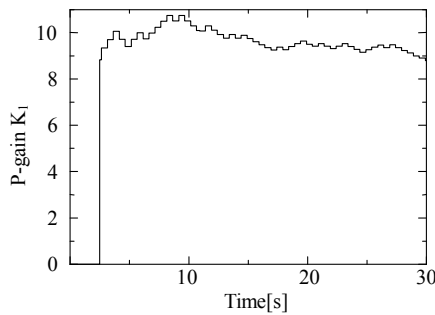


Fig. 11. P-gain versus time.

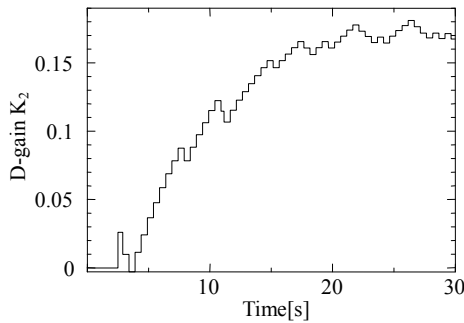


Fig. 12. D-gain versus time.

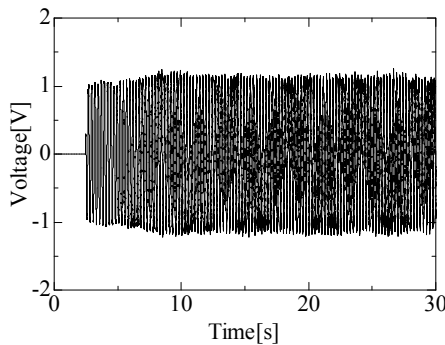


Fig. 13. Control voltage versus time.

These values are close to the values obtained by the trial and errors as mentioned above ( $K_1=8$  and  $K_2=0.18$ ). Therefore, the optimal feedback coefficients will be able to be obtained by the method as just mentioned, when the system parameters are unknown.

#### 4. Conclusions

A new type actuator having characteristics of both spring and actuator was developed, and vibration isolation system was constructed by using the actuator. The results are summarized as follows:

(1) The construction and production method were presented, and it was ascertained that both positive and negative driving were possible for corresponding positive and negative electric currents in the electromagnet.

(2) The method of disturbance cancellation has been presented that requires the sensor for detecting the base, but requires no sensors for the vibrating body. The principle of the control method was presented, and the method for obtaining the optimal feedback coefficient was presented in which the system parameters were not needed in the control.

(3) Vibrations from the base were isolated to be almost zero, which is difficult to be achieved in the normal feedback control. Especially there was no resonance when the present method was applied.

#### References

- [1] Y. Haga, W. Makishi, K. Iwami, K. Totsu, K. Nakamura, M. Esashi, Sensors and Actuators A: Physical **119**(2), 316-322 (2005).
- [2] Qin Chang-jun, Ma Pei-sun, Yao Qin, Sensors and Actuators A: Physical **113**(1), 94-99 (2004).
- [3] J. D. Chiodo, N. Jones, E. H. Billett, D. J. Harrison, Materials & Design **23**(5), 471-478 (2002).
- [4] S. Ikai, K. Ohsawa, K. Nagaya, H. Kashimoto, Journal of Sound and Vibration **231**(2), 393-409 (2000).
- [5] K. Nagaya, H. Kanai, Journal of Sound and Vibration **180-4**, 645-655 (1995).

\*Corresponding author: nagaya420@Yahoo.co.jp